Available online at www.sciencedirect.com
SCIENCE DIRECT®
Carbon 43 (2005) 1857–1863
CARBON
www.elsevier.com/locate/carbon

Cu–Ni composition gradient for the catalytic synthesis of vertically aligned carbon nanofibers

K.L. Klein [a], A.V. Melechko [a,b], P.D. Rack [b], J.D. Fowlkes [b], H.M. Meyer [c], M.L. Simpson [a,b,*]

[a] *Molecular-Scale Engineering and Nanoscale Technologies Research Group, Oak Ridge National Laboratory, P.O. Box 2008, Building 3500, Oak Ridge, TN 37831-6006, USA*
[b] *Department of Materials Science and Engineering, University of Tennessee, Knoxville, TN 37996-2200, USA*
[c] *Microscopy Microanalysis and Microstructures Group, Metals and Ceramics Division, Oak Ridge National Laboratory, Oak Ridge, TN 37831-6064, USA*

Received 8 October 2004; accepted 17 February 2005
Available online 23 March 2005

Abstract

The influence of catalyst alloy composition on the growth of vertically aligned carbon nanofibers was studied using Cu–Ni thin films. Metals were co-sputtered onto a substrate to form a thin film alloy with a wide compositional gradient, as determined by Auger analysis. Carbon nanofibers were then grown from the gradient catalyst film by plasma enhanced chemical vapor deposition. The alloy composition produced substantial differences in the resulting nanofibers, which varied from branched structures at 81%Ni–19%Cu to high aspect ratio nanocones at 80%Cu–20%Ni. Electron microscopy and spectroscopy techniques also revealed segregation of the initial alloy catalyst particles at certain concentrations.

Keywords: Carbon nano-fibers; Chemical vapor deposition; Plasma deposition; Electron microscopy; Catalytic properties

1. Introduction

Vertically aligned carbon nanofibers (VACNFs) prepared by plasma enhanced chemical vapor deposition (PECVD) are of high interest due to their physical properties and nanoscale dimensions [1–5]. Deterministic growth of VACNFs, i.e. precise control of their geometry, location and composition, enables a wide range of applications including electron field emitters [6,7] gene delivery arrays [8,9], synthetic membrane structures [10], electrochemical probes [11,12], and scanning probe tips [13]. The growth of VACNFs is catalytically controlled, thus the choice of catalyst plays a major role in determining the fiber properties [14]. There have been several studies showing that binary or multi-element alloys provide certain advantages over single element catalysts for the growth of filamentous carbon [15]. Whereas transition metals like Ni, Fe, and Co are known to be very active in their ability to break and reform carbon–carbon bonds, other metals such as Cu or Al are relatively non-catalytic but they may affect carbon diffusion and reaction rates [16,17]. In fact, some studies have shown that certain Cu–Ni mixtures have higher catalytic activity than for pure Ni [16,17]. In addition, a 1:1 Cu–Ni sputtered alloy film was found most suitable for low temperature fiber growth [18]. There have also been several reports of Cu–Ni alloys producing multi-directional or branching nanostructures [17,19–21], which may be useful for nanoelectronic wiring or synthetic membrane applications. However, each of the previous studies

* Corresponding author. Fax: +1 865 576 2813.
E-mail addresses: kleinkl@ornl.gov (K.L. Klein), simpsonML1@ornl.gov (M.L. Simpson).

0008-6223/$ - see front matter © 2005 Elsevier Ltd. All rights reserved.
doi:10.1016/j.carbon.2005.02.027

reflect growth from discrete alloy compositions under specific conditions. Even slight variations in catalyst composition can substantially affect fiber composition, growth rate, structure and morphology. Furthermore, the behavior of the catalyst depends on growth conditions such as temperature, source and etchant gas, as well as substrate material [22]. In other words, catalyst composition in combination with the set of growth parameters ultimately determines catalytic performance and the resulting fiber properties.

The control of properties through catalyst selection may be advantageous for tailoring carbon nanofibers to specific applications or for optimizing growth in a particular process. For example, a catalyst for highly branched nanofibers might be desired if high surface area is preferred, while another catalyst could provide small tip diameters useful for field emission or probe devices. Likewise, the process itself may be of utmost importance and certain catalysts are better suited for the desired synthesis parameters such as growth at low temperatures or growth on insulating substrates. An understanding of the relationship between the catalyst material and the resulting fiber growth is vital to selection of the optimal catalyst for each application. Thus, there is need for an efficient method of evaluating a wide range of metallic alloys in order to attain the best catalyst for the given synthesis conditions and desired fiber properties.

The co-sputtered catalyst approach used here, allows for the examination of a large composition space for binary or ternary phase diagrams from a single wafer deposition. The alloy range can also be skewed to span a certain composition range by adjusting the source power and tilt angle of each target. Due to elevated energies, the sputtering technique has the advantage of better mixing and adhesion as compared to evaporated films. In addition, substrate heat and bias capabilities can control film properties such as grain size [23]. Thin sputtered films are also compatible with standard resist patterning.

In this letter we present electron microscopy and spectroscopy analysis of vertically aligned carbon nanofibers synthesized from Cu–Ni alloy catalysts by dc PECVD. A Cu–Ni alloy gradient, with composition varying linearly from 81% Ni to 80% Cu, was prepared by co-sputtering in an RF magnetron sputtering system. The changes in morphology and structure of the resulting carbon nanofibers as well as the level of segregation of catalyst components are investigated at several locations along the composition gradient.

2. Experimental

2.1. Catalyst preparation and composition analysis

First, a binary gradient was created by co-sputtering Cu and Ni targets onto a 100 mm diameter Si(100) wafer using a radio frequency magnetron sputtering system equipped with three 2-inch diameter sputtering sources. For the Cu–Ni catalyst deposition, two sources were used 180° apart, with the substrate centered and equidistant (13.6 cm) relative to the two sources. By varying individual source powers and source tilt angles the gradient slope was adjusted so that the 50–50% atomic ratio was targeted for the middle of the wafer. Based on the sputter yields and predetermined rate data for Cu and Ni, the source powers for Cu and Ni were 100 W and 141 W, respectively. The Cu and Ni sources were sputtered for 1.6 min and the film was about 20 nm thick as predicted by the sputtering rate of 12.5 nm/min. Next, eight collinear points 1 cm apart along the central axis of the wafer were marked and analyzed by scanning Auger microprobe (SAM) in a PHI 680. The composition at each of these points was also verified by energy dispersive X-ray analysis (EDX) in a Hitatchi S-4700.

2.2. Carbon nanofiber synthesis

Then VACNFs were grown on the catalyst gradient film by dc glow discharge PECVD. Upon a 2 min pretreatment at 700 °C in an ammonia plasma, the Cu–Ni thin film broke into nanoparticles which catalyzed the nanofiber growth. Acetylene (C_2H_2) at 25 sccm and ammonia (NH_3) at 80 sccm were used as the carbon source and etchant gases. The sample was grown for 30 min at a pressure of 2.5 Torr, with a current of 150 mA and a bias of 550 V. More details on the apparatus, experimental conditions and carbon nanofiber synthesis can be found elsewhere [4].

2.3. Electron microscopy and spectroscopy analysis

The as-grown sample was characterized at each of the eight points of different catalyst composition by scanning electron microscopy (SEM) in a Hitatchi S-4700. Then fibers were transferred to lacey carbon coated beryllium grids by scraping them from the substrate using a precision razor blade. The fibers on the grids were then analyzed by transmission electron microscopy (TEM; Hitatchi HF-2000) and by scanning transmission electron microscopy (STEM; Hitatchi HD-2000). The STEMs EDX mapping capabilities were utilized to compare the changes in fiber body and catalyst particle compositions across the wafer.

3. Results and discussion

3.1. Catalyst film characterization

Fig. 1 shows the SAM analysis results of the Cu–Ni gradient prior to nanofiber growth. There is a linear composition gradient ranging from about 80% Ni at

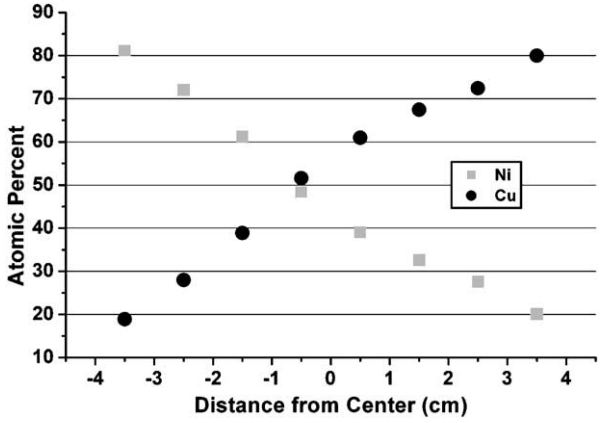

Fig. 1. Auger analysis results for the Cu–Ni gradient showing the atomic percent composition of the catalyst film as a function of position on the substrate.

the first point to 80% Cu at the last point, where the 50–50% atomic ratio fell only a few mm left of center on the wafer. Furthermore, the Auger results closely matched EDX analysis and an empirical sputtering model. The film thickness was verified by atomic force microscopy to be approximately 20 nm.

3.2. Carbon nanofiber characterization

The results of VACNF growth on the Cu–Ni gradient are depicted graphically in Fig. 2. The feature size is the fiber diameter at its widest point as measured from a top view SEM image, implying the average space occupied by a fiber in each area. In some cases this was the breadth of the tips of a branching fiber, or in other cases the span of a broad fiber base was measured. The density of fibers was also calculated from the top view SEM images at each composition point, as the number of fibers in an area of 7 μm^2. As can be seen from Fig. 2(a) and (b), increasing the level of Cu reduced the feature size from roughly 400 nm to 100 nm, while the fiber density increased six-fold. A qualitative analysis of the SEM top view images showed a change in the general shape of the fibers across the gradient from a branchy, random structure to a round uniform structure as the concentration of Cu increases.

In addition, tilted SEM imaging revealed a dramatic decrease in fiber tip diameter, from an average of 57 nm down to 12 nm, with increasing Cu content in the catalyst film (Fig. 2(c)). In Fig. 2(c) it must be noted that for the branched structures on the Ni rich end of the gradient, several tip diameters from each fiber were measured. In contrast, on the Cu-rich side of the gradient where conical fibers with a single tip were produced, only one tip diameter per fiber was measured. This implies that the initial Ni-rich catalyst particles were at least several times larger than 57 nm prior to splitting. Tilted

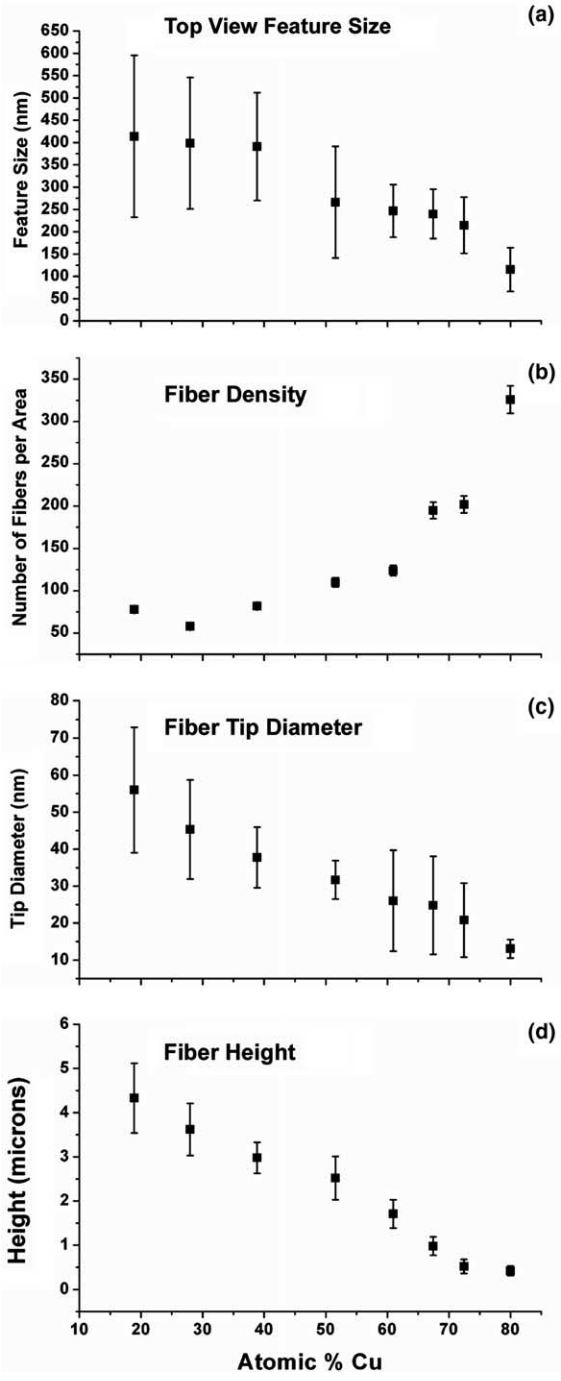

Fig. 2. Graphical trends as Cu content in the catalyst is increased, depicting (a) a decrease in the top view feature size, (b) an increase in fiber density, (c) a reduction of fiber tip diameter and (d) a reduction of fiber height. The standard deviations of each point are shown by the error bars.

SEM images also revealed a sharp decrease in fiber height with increasing Cu concentration (Fig. 2(d)). The drastic reduction of fiber height, or growth rate, with elevated levels of Cu may be due to the low catalytic activity of Cu relative to Ni, which is considered to be the most active metal for carbon catalysis [22].

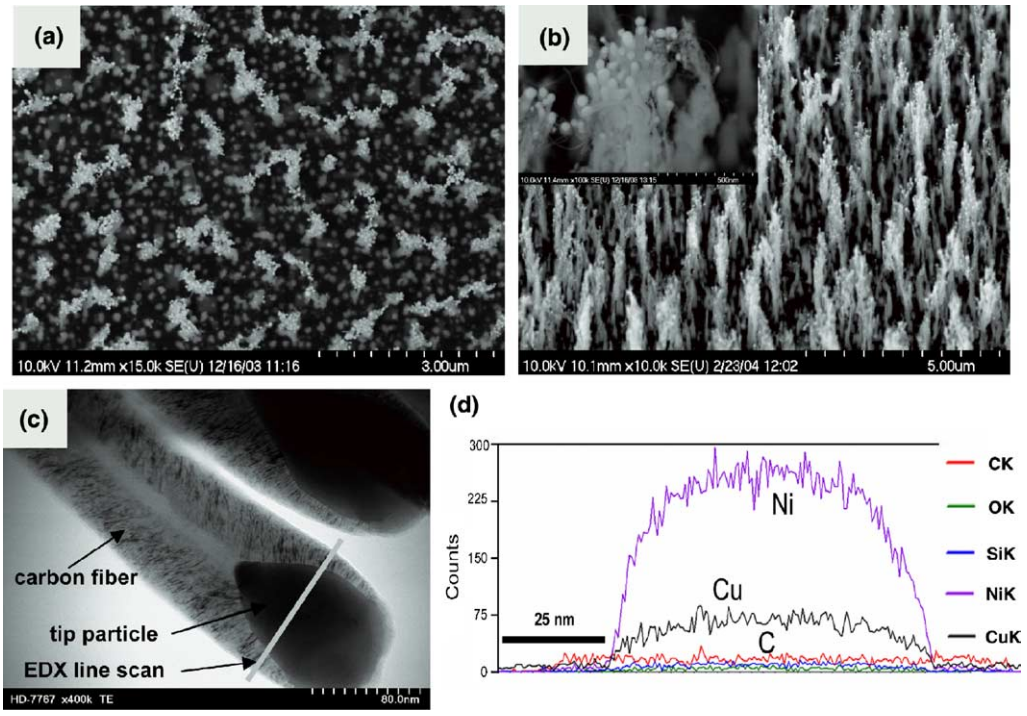

Fig. 3. SEM images of 81%Ni–19%Cu fibers taken at (a) top view and (b) 30° tilt angle with close-up inset of branched fiber tips. A TEM image (c) of the carbon nanofiber tips with EDX line scan across the catalyst particle shown in (d).

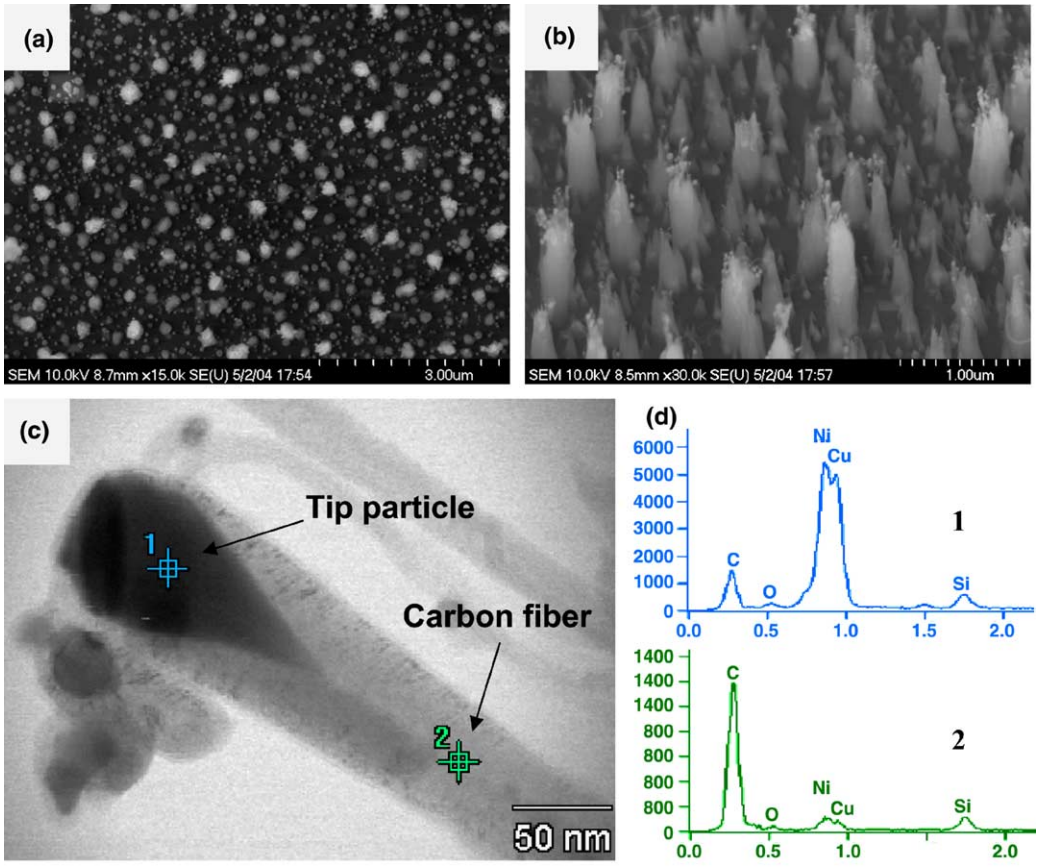

Fig. 4. SEM images of 39%Ni–61%Cu fibers taken at (a) top view and (b) 30° tilt angle. A TEM image (c) of a carbon nanofiber tip with EDX analysis at points labeled 1 and 2 shown in (d).

Images of the resulting VACNFs grown from three different alloy film compositions are shown in Figs. 3 (81% Ni), 4 (39% Ni) and 5 (20% Ni). The 81% Ni rich catalyst grew tall, branched structures with multiple tips as shown in the SEM images in Fig. 3(a) and (b). Branched structures have often been attributed to Cu incorporation in the catalyst [17,19–21,24,25]. However the multidirectional or ''nano-octopus'' structures first observed by Nishiyama et al., and later by many others, exhibit many limbs emanating from a single catalyst particle, presumably in a base-type growth mode [17,19–21,24]. Conversely, in our case Cu alloying with Ni caused the particle to split during tip-type growth. This is similar to Y-junction branching where catalyst splitting can occur from the use of Cu catalysts [25,26], catalyst impurities [27], templates [28] or a rapid drop in temperature during growth [29].

Fig. 3(d) shows EDX line scan analysis at a fiber tip particle where the alloy film composition was 81% Ni. The result demonstrates that the ratio of Ni to Cu stayed at about 81% and therefore there was no segregation of the alloy. However, as the level of Cu increases we observe the alloy segregate, as can be seen in Fig. 4(d). Here the original film was 39% Ni but the fiber tip particles consisted of slightly more Ni than Cu, about 52% Ni. The Cu on the other hand, appears to collect at the base of the growing fiber, where a Cu-rich particle resides. While mostly carbon, residual amounts of metal (throughout) and silicon (increasing abundance near the substrate) were seen in the fiber body.

The SEM images in Fig. 4(a) and (b) illustrate a transition to shorter, more conical, less branched structure. In fact, when Cu levels reach 80% we see dense arrays of uniform, aligned, high aspect ratio cones as shown

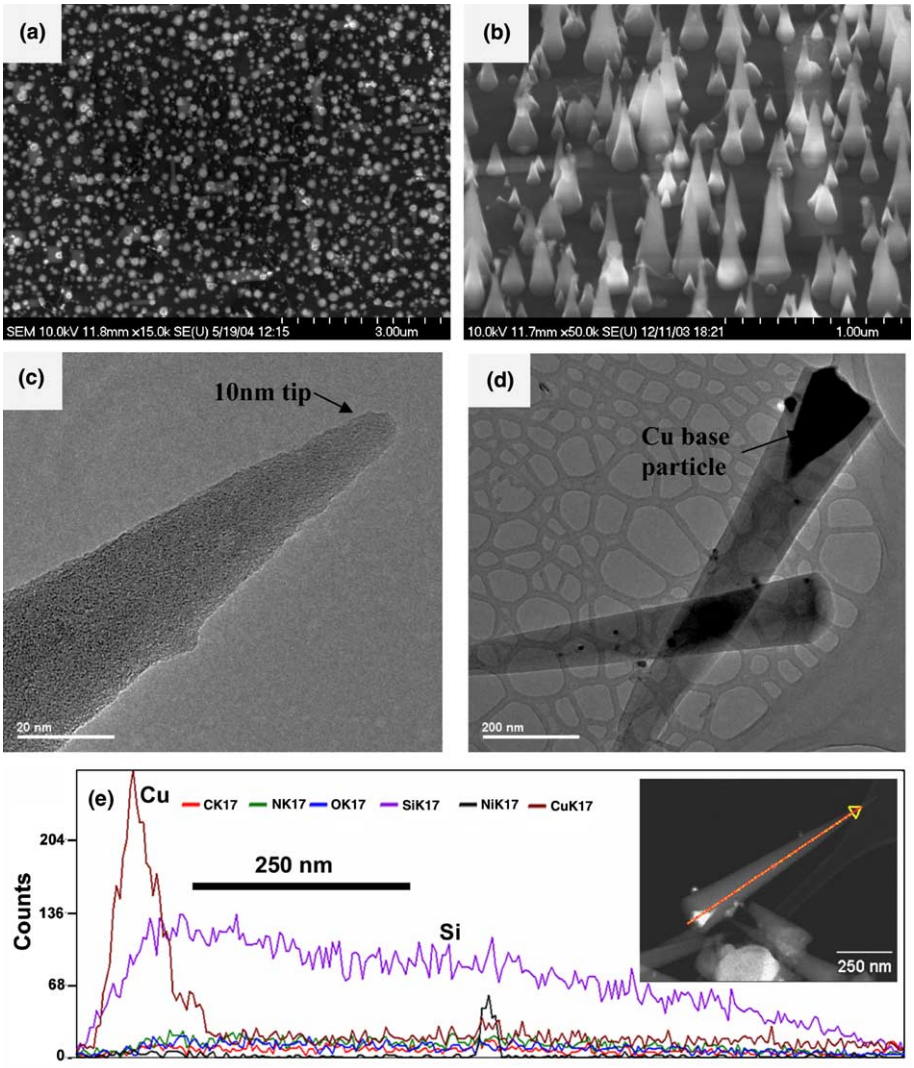

Fig. 5. SEM images of 20%Ni–80%Cu high aspect ratio nanocones taken at (a) top view and (b) 30° tilt angle. TEM images (c) of a 10 nm cone tip and (d) cone with a Cu base particle. The elemental composition of the conical fiber in the lower right can be seen from the EDX line scan (e).

in Fig. 5. High resolution TEM reveals 10 nm tips (Fig. 5(c)) and an average cone angle of 10°. Large characteristic base particles can be seen in Fig. 4(d). EDX revealed that these base particles were entirely Cu as shown in the line scan along the fiber body in Fig. 5(e). The nanocone body itself was composed of an amorphous mixture of Si, C, O, and N. It is unlikely though, that growth occurred primarily from the base particle because of the definitive alignment of the structures, which is a result of tip-type growth [30]. In addition, a small amount of Ni, presumably left over from the segregated alloy, appears to be located at the tips of the fibers. Although, some fibers lack these tip particles, it's possible that they were once there and either diminished due to ion sputtering, were incorporated into the fiber body, or broke off due to an undercutting etch beneath the particle [31]. This unusual structure may be explained by the following sequence: (1) initial Cu and Ni segregation and formation of a small Ni particle; (2) tip-type growth of a thin nanofiber from this Ni particle; (3) continual etching of the nanofiber by the ammonia plasma, but before complete etching (4) encapsulation of the nanofiber within a sheath composed of a silicon–nitride–oxide mixture formed from substrate sputtering and the plasma gases [32]. The fact that the cones without tip particles still remain sharp in the plasma environment is a testament to the resilience of this the material to etching, seeing as how pure carbon fibers under these plasma conditions would be eroded without the etch-mask of a tip particle. This type of fiber may be of interest due to its high aspect ratio, small tip size and robust outer coating.

4. Conclusions

Catalyst particles play a critical role in the deterministic growth of carbon nanofibers. Previous studies have indicated that alloy catalysts can have certain advantages over traditional single element catalysts. In order to find the optimal catalyst for each application an efficient method to assess a wide range of metallic alloys for carbon nanofiber synthesis was needed.

A co-sputtered Cu–Ni gradient was used to evaluate carbon nanofiber growth over a wide composition range. The results show substantial changes in fiber composition, growth rate, structure and morphology across the gradient. As the concentration of Cu increased, general growth trends include: a reduction of feature size, slower growth rate, morphological change from branching fibers to uniform cones, increased incorporation of Si in the fiber sidewalls, and segregation of the alloy catalyst with the formation of a Cu base particle. Explanation of the growth modes for branched structures and conical structures were proposed.

Furthermore, co-sputtered gradient films can be used to evaluate and optimize carbon nanofiber growth of other multi-metal alloys. These gradient films are applicable to the diverse parameters of both CVD and PECVD systems. Since PECVD conditions used for VACNF growth differ significantly from conditions for thermal CVD nanofiber growth, catalyst performance should be evaluated for each. From this type of study, a catalyst composition can be rapidly optimized for any growth system and the desired fiber qualities.

Acknowledgments

MLS acknowledges support from the Material Sciences and Engineering Division Program of the DOE Office of Science under contract DE-AC05-00OR22725 with UT-Battelle LLC, and KLK acknowledges support from the Center for Nanophase Materials Sciences (CNMS) Research Scholar Program. Additional support was provided by the Defense Advanced Research Projects Agency (DARPA) under Contract No. DE-AC05-00OR22725. Scanning Auger Microanalysis was sponsored by the Assistant Secretary for Energy Efficiency and Renewable Energy, Office of FreedomCAR and Vehicle Technologies, as part of the High Temperature Materials Laboratory User Program, ORNL, managed by UT-Battelle, LLC, for the US Department of Energy under contract number DE-AC05-00OR22725.

References

[1] Ren ZF, Huang ZP, Xu JW, Wang JH, Bush P, Siegal MP, et al. Synthesis of large arrays of well-aligned carbon nanotubes on glass. Science 1998;282(5391):1105–7.
[2] Ren ZF, Huang ZP, Wang DZ, Wen JG, Xu JW, Wang JH, et al. Growth of a single freestanding multiwall carbon nanotube on each nanonickel dot. Appl Phys Lett 1999;75(8):1086–8.
[3] Chhowalla M, Teo KBK, Ducati C, Rupesinghe NL, Amaratunga GAJ, Ferrari AC, et al. Growth process conditions of vertically aligned carbon nanotubes using plasma enhanced chemical vapor deposition. J Appl Phys 2001;90(10):5308–17.
[4] Merkulov VI, Hensley DK, Melechko AV, Guillorn MA, Lowndes DH, Simpson ML. Control mechanisms for the growth of isolated vertically aligned carbon nanofibers. J Phys Chem B 2002;106(41):10570–7.
[5] Merkulov VI, Lowndes DH, Wei YY, Eres G, Voelkl E. Patterned growth of individual and multiple vertically aligned carbon nanofibers. Appl Phys Lett 2000;76(24):3555–7.
[6] Guillorn MA, Yang X, Melechko AV, Hensley DK, Hale MD, Merkulov VI, et al. Vertically aligned carbon nanofiber-based field emission electron sources with an integrated focusing electrode. J Vacuum Sci Technol B 2004;22(1):35–9.
[7] Merkulov VI, Lowndes DH, Baylor LR. Scanned-probe field-emission studies of vertically aligned carbon nanofibers. J Appl Phys 2001;89(3):1933–7.

[8] McKnight TE, Melechko AV, Hensley DK, Mann DGJ, Griffin GD, Simpson ML. Tracking gene expression after DNA delivery using spatially indexed nanofiber arrays. NanoLetters 2004;4(7): 1213–9.
[9] McKnight TE, Melechko AV, Griffin GD, Guillorn MA, Merkulov VI, Serna F, et al. Intracellular integration of synthetic nanostructures with viable cells for controlled biochemical manipulation. Nanotechnology 2003;14(5):551–6.
[10] Zhang L, Melechko AV, Merkulov VI, Guillorn MA, Simpson ML, Lowndes DH, et al. Controlled transport of latex beads through vertically aligned carbon nanofiber membranes. Appl Phys Lett 2002;81(1):135–7.
[11] McKnight TE, Melechko AV, Austin DW, Sims T, Guillorn MA, Simpson ML. Microarrays of vertically-aligned carbon nanofiber electrodes in an open fluidic channel. J Phys Chem B 2004; 108(22):7115–25.
[12] Guillorn MA, McKnight TE, Melechko A, Merkulov VI, Britt PF, Austin DW, et al. Individually addressable vertically aligned carbon nanofiber-based electrochemical probes. J Appl Phys 2002;91(6):3824–8.
[13] Ye Q, Cassell A, Liu H, Chao K-J, Han J, Meyyappan M. Large-scale fabrication of carbon nanotube probe tips for atomic force microscopy critical dimension imaging applications. NanoLetters 2004;4(7):1301.
[14] Zaginaichenko SY, Schur DV, Matysina ZA. The peculiarities of carbon interaction with catalysts during the synthesis of carbon nanomaterials. Carbon 2003;41(7):1349–55.
[15] Kichambare PD, Qian D, Dickey EC, Grimes CA. Thin film metallic catalyst coatings for the growth of multiwalled carbon nanotubes by pyrolysis of xylene. Carbon 2002;40(11): 1903–9.
[16] Kim MS, Rodriguez NM, Baker RTK. The interaction of hydrocarbons with copper–nickel in the formation of carbon filaments. J Catal 1991;131:60–73.
[17] Nishiyama Y, Tamai Y. Carbon formation on copper–nickel alloys from benzene. J Catal 1974;33:98–107.
[18] Kamada K, Ikuno T, Takahashi S, Oyama T, Yamamoto T, Kamizono M, et al. Surface morphology and field emission characteristics of carbon nanofiber films grown by chemical vapor deposition on alloy catalyst. Appl Surf Sci 2003;212: 383–7.
[19] Avdeeva LB, Goncharova OV, Kochubey DI, Zaikovskii VI, Plyasova LM, Novgorodov BN, et al. Coprecipitated Ni-alumina and Ni–Cu-alumina catalysts of methane decomposition and carbon deposition. 2. Evolution of the catalysts in reaction. Appl Catal A—General 1996;141(1–2):117–29.
[20] Bernardo CA, Alstrup I, Rostrup-Nielsen JR. Carbon deposition and methane steam reformation on silica-supported Ni–Cu catalysts. J Catal 1985;96:517–34.
[21] Pradhan D, Sharon M, Kumar M, Ando Y. Nano-octopus: a new form of branching carbon nanofiber. J Nanosci Nanotechnol 2003;3(3):215–7.
[22] Cassell AM, Ye Q, Cruden BA, Li J, Sarrazin PC, Ng HT, et al. Combinatorial chips for optimizing the growth and integration of carbon nanofibre based devices. Nanotechnology 2004;15(1):9–15.
[23] Choi YC, Shin YM, Lim SC, Bae DJ, Lee YH, Lee BS, et al. Effect of surface morphology of Ni thin film on the growth of aligned carbon nanotubes by microwave plasma-enhanced chemical vapor deposition. J Appl Phys 2000;88(8):4898–903.
[24] Chambers A, Rodriguez NM, Baker RTK. Influence of copper on the structural characteristics of carbon nanofibers produced from the cobalt-catalyzed decomposition of ethylene. J Mater Res 1996;11(2):430–8.
[25] Gan B, Ahn J, Zhang Q, Yoon SF, Rusli, Huang QF, et al. Branching carbon nanotubes deposited in HFCVD system. Diamond Relat Mater 2000;9(3–6):897–900.
[26] Deepak FL, Govindaraj A, Rao CNR. Synthetic strategies for Y-junction carbon nanotubes. Chem Phys Lett 2001;345(1–2):5–10.
[27] Li WZ, Wen JG, Ren ZF. Straight carbon nanotube Y junctions. Appl Phys Lett 2001;79(12):1879–81.
[28] Li J, Papadopoulos C, Xu J. Nanoelectronics—growing Y-junction carbon nanotubes. Nature 1999;402(6759):253–4.
[29] Teo KBK, Singh C, Chhowalla M, Milne WI. Catalystic synthesis of carbon nanotubes and nanofibers. In: Nalwa HS, editor. Encyclopedia of nanoscience and nanotechnology. American Scientific Publishers; 2003. p. 1–22.
[30] Merkulov VI, Melechko AV, Guillorn MA, Lowndes DH, Simpson ML. Alignment mechanism of carbon nanofibers produced by plasma-enhanced chemical-vapor deposition. Appl Phys Lett 2001;79(18):2970–2.
[31] Merkulov VI, Melechko AV, Guillorn MA, Lowndes DH, Simpson ML. Sharpening of carbon nanocone tips during plasma-enhanced chemical vapor growth. Chem Phys Lett 2001; 350(5–6):381–5.
[32] Melechko AV, McKnight TE, Guillorn MA, Merkulov VI, Ilic B, Doktycz MJ, et al. Vertically aligned carbon nanofibers as sacrificial templates for nanofluidic structures. Appl Phys Lett 2003;82(6):976–8.